Optics Letters

Room temperature mid-infrared fiber lasing beyond 5 μm in chalcogenide glass small-core step index fiber

J. J. Nunes,[1,*] Ł. Sojka,[2] R. W. Crane,[1] D. Furniss,[1] Z. Q. Tang,[1,3] D. Mabwa,[1] B. Xiao,[1] T. M. Benson,[1] M. Farries,[1] N. Kalfagiannis,[4] E. Barney,[1] S. Phang,[1] A. B. Seddon,[1,5] and S. Sujecki[2]

[1]Mid-Infrared Photonics Group, George Green Institute for Electromagnetics' Research, Faculty of Engineering, University of Nottingham, Nottingham NG7 2RD, UK
[2]Department of Telecommunications and Teleinformatics, Faculty of Electronics, Wroclaw University of Science and Technology, Wybrzeze Wyspianskiego 27, 50-370 Wroclaw, Poland
[3]Fibercore Limited, Fibercore House, Southampton Science Park SO16 7QQ, UK
[4]School of Science and Technology, Nottingham Trent University, Nottingham NG11 8NS, UK
[5]e-mail: angela.seddon@nottingham.ac.uk
*Corresponding author: eexjn6@exmail.nottingham.ac.uk

Received 7 May 2021; revised 27 May 2021; accepted 27 May 2021; posted 3 June 2021 (Doc. ID 430891); published 19 July 2021

This Letter, to the best of our knowledge, reports mid-infrared fiber lasing beyond 5 μm at room temperature for the first time, Ce^{3+}-doped, chalcogenide glass, step index fiber employed in-band pumping with a 4.15 μm quantum cascade laser. The lasing fiber is was 64 mm long, with a calculated numerical aperture of 0.48 at the lasing wavelengths. The core glass was $Ge_{15}As_{21}Ga_1Se_{63}$ atomic % (at. %), doped with 500 parts-per-million-by-weight Ce, with a 9 μm core diameter. The cladding glass was $Ge_{21}Sb_{10}Se_{69}$ at. % with a 190 μm outer diameter. As pump power increases continuous wave lasing corresponding to the $^2F_{7/2} \rightarrow {}^2F_{5/2}$, transition in the Ce^{3+} ion occurs at 5.14 μm, 5.17 μm, and 5.28 μm.

https://doi.org/10.1364/OL.430891

The mid-infrared region (MIR; defined as 3–50 μm in [1]) enables direct molecular sensing with high selectivity/specificity. MIR fiber lasers offer excellent beam quality of bright, spatially and temporally coherent light, routable in MIR fiber-optics for applications such as narrow-band sensing, clinical diagnostics, new medical laser wavelengths, and pulsed seeding of MIR-supercontinua for MIR broadband sensing [2].

The longest wavelength room temperature continuous wave (CW) fiber lasing to date is 3.92 μm in Ho^{3+}-doped fluoro-indate glass fiber [3], enabled by the lower phonon energy [4] (509 cm^{-1}) fluoro-indate glass host compared to prior fluoro-zirconate glass hosts. However, 509 cm^{-1} is still too high for laser operation > 4 μm [5]; thus, chalcogenide glass hosts, with phonon energies down to 200 cm^{-1}, are prime candidates [6] to achieve this goal. Selenide-chalcogenide glasses sufficiently combine low phonon energy with good glass stability.

Covalent chalcogenide glasses exhibit large linear refractive indices, so large absorption/emission cross-sections of doped-in lanthanide-ions provide promising short, active devices. Chalcogenide glasses are based on sulfur S, selenium Se, and tellurium Te; thus, adding Groups 14 and 15 elements increases chemical/mechanical robustness. Chalcogenide fibers are weaker than silica fibers, exhibiting a Young's modulus of ~ 1/5 x silica [7] and a Vickers' hardness of ~ 2 GPa [8] (cf. window-glass: 5.5 GPa). Chalcogenide glasses/fiber are exceptionally stable in liquid water/water–vapor at ambient temperature, unlike fluoride glasses [9], and they are not oxidized in air below the glass transition temperature, beyond a protective oxide nanolayer [10] analogous to ambient silicon oxidation [11]. Plastic-coated/uncoated chalcogenide fibers older than 2 years, stored under ambient conditions, retained respectable ultimate fracture stress median of ~ 80 MPa [12]. Coated/uncoated fibers can maintain optical transmission for over 7 years. Furthermore, high optical damage thresholds have also been reported [13].

The MIR-PL (photoluminescence) emission of lanthanide ions in selenide glasses occurs across the wavelengths 3–10 μm [14]. Calculated non-radiative transition rates are orders of magnitude lower than fluoride glasses [15], and hence, they offer higher efficiencies and lower thermal problems. We reported first-step index Pr^{3+}-doped chalcogenide fiber MIR-PL emission, and long milli-second MIR-PL lifetime equivalent to bulk-glass, showing fiber processing had not compromised the lanthanide local environment [16]. With Churbanov and Shiryaev [17], we demonstrated record low optical loss GeAsSe fiber. Recently, we have announced gain in Pr^{3+}-doped selenide fiber [18]. In addition, Tb^{3+} and Pr^{3+} doped chalcogenide bulk

glass lasers have been reported [19,20]. However, the multiple excitation levels of Tb^{3+} and Pr^{3+} give rise to excited state absorption at some wavelengths, and this can reduce population inversion.

In this Letter, we report MIR fiber lasing $> 5\,\mu m$ in a step-index selenide–chalcogenide fiber. The step index fiber comprised core glass: 500 ppmw (parts-per-million-by-weight) Ce -$Ge_{15}As_{21}Ga_1Se_{63}$ at. % and cladding glass $Ge_{21}Sb_{10}Se_{69}$ at. %. The Ce^{3+} ion dopant was selected due to its simple energy level structure, which, in principle, excludes excited state absorption and co-operative up-conversion phenomena, while allowing efficient in-band pumping, with a small quantum defect. Thus, this choice mimics Yb^{3+}-doped silica glass, both reducing heating in the cavity and with potential for becoming the MIR analogue of the Yb^{3+}-doped silica glass fiber laser. This contribution, besides reporting the MIR fiber lasing beyond 5 μm also displays results on Ce^{3+} MIR-PL.

To create the step index lasing fiber, arsenic As (7N5, Furakawa Denshi), antimony Sb (5 N, Materion), and selenium Se (5N, Materion) were heated under vacuum (10^{-3} Pa), to remove anionic impurities; germanium Ge (5N, Cerac) was used as supplied. Melt-containment was a silica glass ampoule, purified by heating at 1000°C/6 h (hours), first in air (removed carbonaceous impurities), then in vacuum (10^{-3} Pa) (removed physi-/chemi-sorbed water). Precursors were batched under N_2 gas (MBraun Glovebox: < 1 ppm O_2; < 1 ppm H_2O). Cladding glass, $Ge_{21}Sb_{10}Se_{69}$ at. %. (M287RC), was melted at 900°C/12 h. Core-glass constituents 0.99 ($Ge_{15}As_{21}Se_{63}$) at. % were pre-melted at 850°C/12 h. Glasses were quenched and annealed, in situ inside the ampoule. The $Ge_{21}Sb_{10}Se_{69}$ at. %. cladding glass was then extruded [2] to form a tube (E093RC) of 10.22 mm outside diameter (OD), inside diameter 900 μm and 60 mm long. The pre-melted core glass 0.99 ($Ge_{15}As_{21}Se_{63}$) at. % had gallium Ga (1 at. %, 3 N purity, Alfa Aesar) plus 500 ppmw Ce foil (3 N, Alfa Aesar) batched on and remelted at 850°C/6 h, then quenched/annealed, to make the 500 ppmw Ce-doped $Ge_{15}As_{21}Ga_1Se_{63}$ at. % core-glass rod preform (M259REZQT), which was drawn to unstructured fiber (F109REZQT(RCJN)), termed intermediate fiber, and it had a 900 μm diameter cane. To fabricate the step index lasing fiber (F130RERC), a rod-in-tube [16] preform was fiber drawn in a radio frequency furnace on a customized heathway fiber-drawing tower within a class-10,000 cleanroom (e.g., see [16]).

Churbanov *et al.* in [21] reported absorption across $1666 - 2857\,cm^{-1}$ (3.5-6 μm) due to the $^2F_{5/2} \rightarrow {}^2F_{7/2}$ transition of Ce^{3+} doped in GeSbGaSe glass. In this work, an absorption spectrum of the core bulk glass [Fig. 1(a)] was collected, 500 ppmw Ce-GeAsGaSe using a Fourier transform infrared (FTIR) spectrometer (Bruker IFS 66/S). The sample pathlength was 2.45 mm.

From Fig. 1(a), the Ce^{3+} absorption due to $^2F_{5/2} \rightarrow {}^2F_{7/2}$ is centered at 4.63 μm ($2160\,cm^{-1}$) and spans $1660 - 2900\,cm^{-1}$ (3.5–6 μm) agreeing well with [21]; the Ce^{3+} absorption band was used to construct the corresponding Ce^{3+} energy level diagram [Fig. 1(b)], which matches the classic Dieke and Crosswhite [22] energy level diagram of Ce^{3+} [Xe] $4f^1$ with the $^2F_{5/2}$ ground state and $^2F_{7/2}$ first excited state separated by $\sim 2200\,cm^{-1}$. The Ce^{3+} electronic absorption overlies [-Se-H] host impurity vibrational absorption [23]. Churbanov et al. in [21] reported MIR PL emission due to

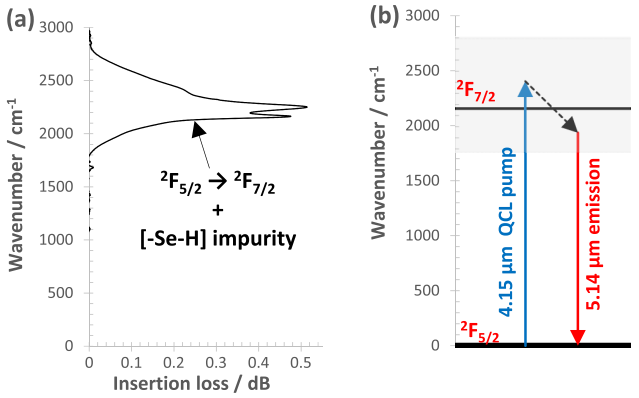

Fig. 1. (a) MIR absorption spectrum of 500 ppmw Ce-doped GeAsGaSe bulk core glass, and (b) Ce^{3+} electronic energy level diagram overlaid with the 4.15 μm QCL and 5.14 μm emission.

$^2F_{7/2} \rightarrow {}^2F_{5/2}$ of Ce^{3+}, in a Ce^{3+}/Dy^{3+} co-doped GeSbGaSe bulk glass, which was broad with two maxima at 4.44 and 4.62 μm of very high absorption cross-section: 4.1×10^{-20} and $3.4 \times 10^{-20}\,cm^2$, respectively. Cross-sections in the present work are not included due to underlying [-Se-H] absorption and potential Ce^{4+} presence. Further work is required to obtain the true Ce^{3+} cross-section.

Ce^{3+} MIR-PL emission from the 500 ppmw Ce-doped GeAsGaSe intermediate fiber was evaluated using in-band pumping with a 4.15 μm quantum cascade laser (QCL), with the equipment configuration shown in Fig. 2(a). Further details on equipment and Ce^{3+} MIR-PL will be discussed in a follow-up paper. From Fig. 2(b), Ce^{3+} PL spanned 3.4–6 μm. A Ce^{3+} MIR-PL lifetime of 3.6 ms was measured at wavelengths 3.8, 4.6, and 5.2 μm, compared to Ce^{3+} PL lifetime 2.5 ms in [21].

The optical loss spectrum of the 500 ppmw Ce doped GeAsGaSe intermediate glass fiber with an OD 246 ± 8 μm and 2.75 m long was collected using the cutback method. From Fig. 3, the Ce^{3+} electronic absorption due to $^2F_{5/2} \rightarrow {}^2F_{7/2}$ overlays vibrational absorption due to hydride impurity in the glass host [cf. Fig. 1(a)]. The lowest optical loss was 2.16 dB m^{-1} across the 6.6–7.1 μm wavelength.

The refractive index dispersion of bulk annealed core and cladding glass samples, which constituted the core and cladding of the step index lasing fiber, were measured on an ellipsometer (Woollam IR-VASE Ellipsometer Mark II). Variable angle spectrometric ellipsometry (V.A.S.E) was employed on the bulk samples at angles of 55°, 65°, and 75°, and models fitted (see Fig. 4). The calculated NA of the lasing fiber was 0.471 at the pump wavelength and 0.476 in the lasing wavelength range.

An unannealed, step-index fiber, with a 500 ppmw Ce-doped GeAsGaSe core with a 9 μm diameter, and 180 μm GeSbSe OD cladding that was 64-mm-long with ~90° cleaved-end faces, was prepared. It was mounted to a stainless-steel V-groove with ultraviolet cured polymer and coated with a metal alloy (Galinstan: InGaSn alloy) for thermal management and cladding mode stripping. A 4.421 μm short wave-pass (SWP; 87 % reflective, and 0.2% transmission at the lasing wavelengths) was abutted to the fiber, while a gold mirror (95.8% reflective at the lasing wavelengths) was abutted to the opposite end, forming the optical cavity (see Fig. 5). A 4.15 μm QCL beam was passed through a polarizer, and a one-fourth wave

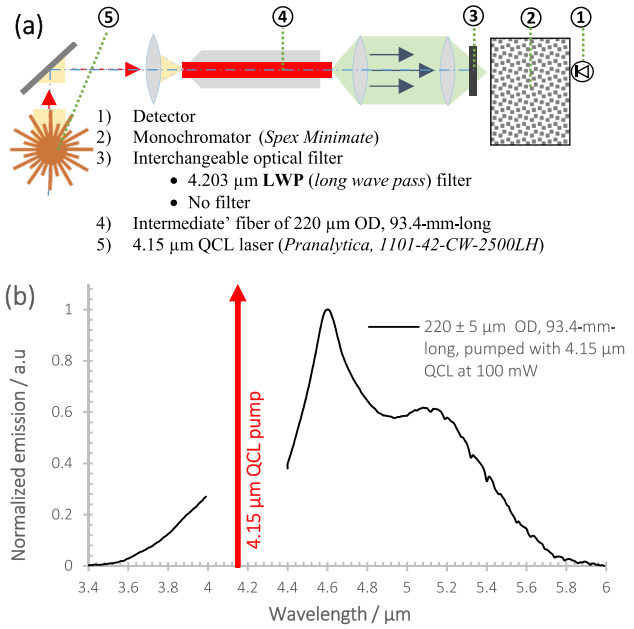

Fig. 2. (a) Simplified equipment diagram used for Ce^{3+} PL (photoluminescence) measurements, and (b) Ce^{3+} MIR-PL emission spectrum of 500 ppmw Ce-doped "intermediate" fiber. Note: A 4.203 μm LWP filter was used ≥ 4.4 μm, and no filter was used at ≤ 3.90 μm.

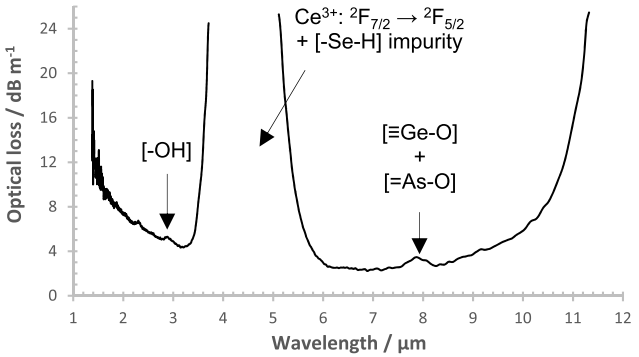

Fig. 3. MIR optical loss of 500 ppmw Ce-doped "intermediate" fiber with an OD = 246 ± 8 μm and length of 2.75 m. The core of the step index lasing fiber has potentially the same optical loss.

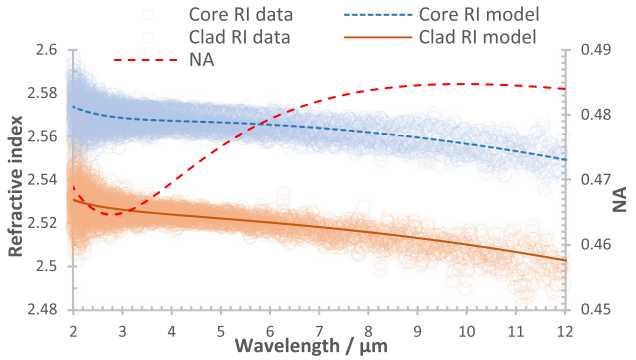

Fig. 4. Refractive index dispersion and V.A.S.E. model plots of bulk glasses. Core: 500 ppmw Ce-doped GeAsGaSe; cladding: GeSbSe.

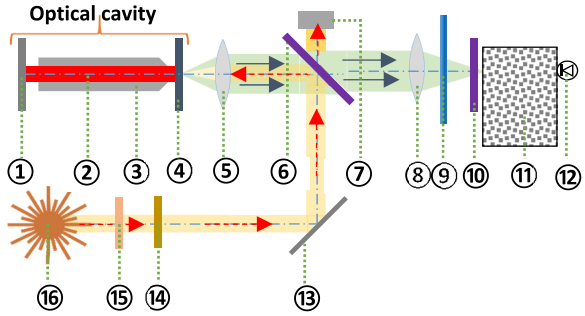

1) Gold mirror (*Thorlabs, ME1-M01*), $R_{@5.14\ \mu m}$ = 95.8 %
2) 9 μm core, 190 μm OD, 64-mm-long filter, coated with InGaSn alloy
3) Stainless steel V-groove fiber holder
4) 4.421 μm SWP (*short wave pass*) filter (*Northumbria Optical Coatings Ltd (NOC), SWP-17220-1-1-17*), $R_{@5.14\ \mu m}$ = 87 %, $T_{@5.14\mu m}$ = 0.2 %
5) Bi-convex CaF_2 (*calcium fluoride*) lens, f = 15 mm (*Thorlabs, LB5766-E*)
6) 4.203 μm LWP (*long wave pass*) filter (*NOC, SLWP-4203-001138*)
7) Thermal power meter (*Thorlabs, C-Series S302C*)
8) CaF_2 lens, f = 50 mm (*Thorlabs, LA5763*)
9) Mechanical chopper (*Bentham Instruments*)
10) 4.630 μm LWP filter (*NOC, SLWP-4630-000434*)
11) Monochromator (*Spex Minimate*) with a 0.25 mm entrance and exit slits, equipped with diffraction grating blazed at 6 μm with a spectral resolution of ~15 nm. Interior purged with dry, atmosphere
12) Mercury cadmium telluride detector (*Vigo Systems, PVI-4TE-6*)
13) Gold mirror (*Thorlabs, ME1-M01*)
14) One-fourth wave plate (*Thorlabs, WPLQ05M-4000*)
15) Polarizer (*Thorlabs, LPMIR050-MP2*)
16) 4.15 μm QCL laser (*Pranalytica, 1101-42-CW-2500LH*) operated in either CW or electronically modulated

Fig. 5. Unoptimized optical setup used to investigate lasing.

plate to prevent reflections and unpolarized Ce^{3+} PL, emanating from the lasing fiber, influencing QCL output power. A 4.203 μm LWP filter was used as a dichroic mirror to reflect the 4.15 μm QCL pump toward the optical cavity. The QCL was then focused through the 4.421 μm SWP filter to the 9 μm core (~ 19% coupling efficiency). The output of the cavity was passed through a 4.630 LWP filter to block the 4.15 μm QCL pump light reflected from the optical cavity. The MIR output spectrum of the cavity was measured to a spectral resolution of ~ 15 nm, using a monochromator and a mercury cadmium telluride detector (Vigo Systems, PVI-4TE-6). The total output power of the cavity was < 100 μW (due to poor transmission of 4.421 μm SWP filter), and it could not be accurately measured with a thermal power meter (Thorlabs, C-Series S302C). The QCL was operated in either CW output, to measure the MIR output spectrum, or electronically with a 50% duty cycle, to measure the cavity "fall time." As the CW pump power increased to 40 mW, initially, CW lasing was observed at 5.13 μm, 5.17 μm, and 5.28 μm, that is, peaks A, B, and C, respectively.

Figure 6 shows the cavity emission spectrum with increasing pump power. Peaks A and B shifted slightly to longer wavelengths as pump power increased. Above the pump power of 86 mW, the intensity of peak A (but not B and C) grew roughly linearly with increasing pump power, while above 400 mW pump power, peak B plateaus and peak C drops to zero. A cavity fall time of 2.5 μs was measured at the 5.127 μm wavelength.

Figure 7 shows the area under laser peaks A, B, and C as the pump power increases. The area under "Peak A," and Total area under peaks A, B, and C both exhibit a near-linear dependence with increasing pump power > 86 mW.

The MIR electronic configuration of Ce^{3+} is [Xe] $4f^1$, with the $^2F_{5/2}$ ground state and $^2F_{7/2}$ excited state. Crystal field and spin-orbit interactions split these two states into three and four

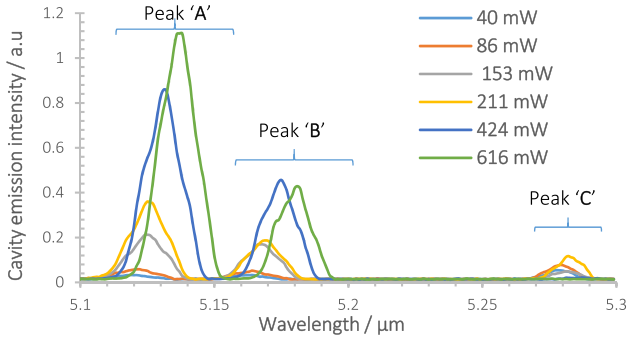

Fig. 6. Cavity emission intensity versus the 500 ppmw Ce-doped GeAsGaSe core that was 9 μm in diameter and 64 mm long for different CW 4.15 μm QCL pump powers.

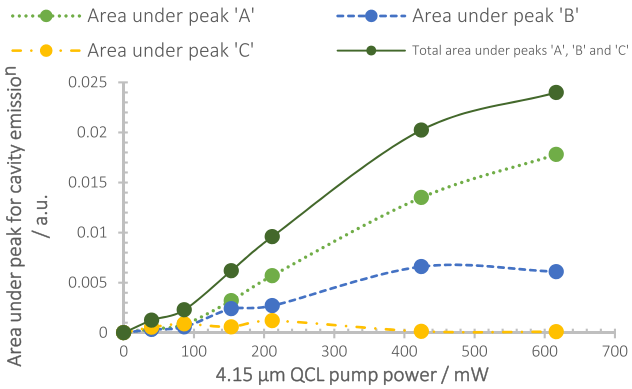

Fig. 7. Areas under cavity emission peaks from Fig. 6 plotted versus the 4.15 μm QCL pump power (mW) of small-core, step index fiber excited with the 4.15 μm CW QCL between 0 and 616 mW.

energy levels, respectively [24,25]. Ce^{3+}-doped glasses and crystals have been investigated as UV-pumped blue lasers [26]. Low-temperature, MIR absorption measurements of Ce^{3+} doped into garnet [24] showed large splitting of the excited $^2F_{7/2}$ up to $\sim 4000\ cm^{-1}$. The theoretical crystal field analysis supported this [25] with 4f–4f intra-shell transitions of Ce^{3+} ions spectrally extending to $\sim 3700\ cm^{-1}$ due to the large splitting of the $^2F_{7/2}$ excited state.

Thermal population of the second Stark level of the $^2F_{5/2}$ ground state was shown to occur at ambient temperature, called "hot" transitions [25]. Here, we observe more than one MIR lasing line; the Stark intra-levels of the upper/lower states may account for the co-existent lasing lines. The Er^{3+}: ZBLAN operated on several wavelength lines in the 2.71–2.79 μm range [27].

In summary, the narrow peaks, short cavity lifetime, the threshold at the 86 mW pump power, and the near-linear dependence with increasing pump power are all evidence of fiber lasing > 5 μm.

Funding. Ministerstwo Nauki i Szkolnictwa Wyższego (IP0441/IP2/2015/73); Royal Society (IES\R3\183055); Engineering and Physical Sciences Research Council (EP/P013708/1, EP/T010762/1).

Acknowledgment. We acknowledge networking support from EU COST Action: MP1401. Authors thank F. Maes and M. Bernier of COPL, Laval University, Canada, for Royal Society funded visit to Nottingham, Oct. 2019, and much insight into fiber cavities.

Disclosures. Authors declare no conflicts of interest.

Data Availability. Digital data underlying analogue results may be obtained from authors upon reasonable request.

REFERENCES

1. "Optics and photonics. Spectral bands," BS ISO 20473:2007 (2007).
2. A. B. Seddon, *Springer Handbook Glass*, J. D. Musgraves, J. Hu, and L. Calvez, eds. (Springer 2019).
3. F. Maes, V. Fortin, S. Poulain, M. Poulain, J.-Y. Carrée, M. Bernier, and R. Vallée, Optica **5**, 761 (2018).
4. R. M. Almeida, J. C. Pereira, Y. Messaddeq, and M. A. Aegerter, J. Non-Cryst. Solids **161**, 105 (1993).
5. A. B. Seddon, Z. Tang, D. Furniss, S. Sujecki, and T. M. Benson, Opt. Express **18**, 26704 (2010).
6. A. B. Seddon, J. Non-Cryst. Solids **184**, 44 (1995).
7. J. S. Sanghera, Naval Research Laboratory (personal communication, 2005).
8. J.-P. Guin, T. Rouxel, J.-C. Sanglebœuf, and J. Lucas, J. Am. Ceram. Soc. **85**, 1545 (2002).
9. A. B. Seddon, *Fluoride Glasses*, A. E. Comyns, ed. (Wiley, 1989), Chap. 7.
10. P. Lucas, A. A. Wilhelm, M. Videa, C. Boussard-Plédel, and B. Bureau, Corros. Sci. **50**, 2047 (2008).
11. M. Morita, T. Ohmi, E. Hasegawa, M. Kawakami, and M. Ohwada, J. Appl. Phys. **68**, 1272 (1990).
12. A. Abdullatif and A. Shah, *Undergraduate Project Reports* (University of Nottingham, 2010).
13. A. Sincore, J. Cook, F. Tan, A. El Halawany, A. Riggins, L. Shah, A. Abouraddy, M. Richardson, and K. Schepler, in *Laser Congress (ASSL, LAC)*, OSA technical digest (Optical Society of America, 2017), paper ATu5A.5.
14. L. B. Shaw, B. Cole, P. A. Thielen, J. S. Sanghera, and I. D. Aggarwal, IEEE J. Quantum Electron. **37**, 1127 (2001).
15. A. B. Seddon, Ł. Sójka, D. Furniss, Z. Tang, R. Crane, J. Nunes, S. Phang, E. Barney, M. Farries, T. M. Benson, and S. Sujecki, Proc. SPIE **11635**, 1163503 (2021).
16. Z. Tang, D. Furniss, M. Fay, H. Sakr, L. Sójka, N. Neate, N. Weston, S. Sujecki, T. M. Benson, and A. B. Seddon, Opt. Mater. Express **5**, 870 (2015).
17. Z. Tang, V. S. Shiryaev, D. Furniss, L. Sojka, S. Sujecki, T. M. Benson, A. B. Seddon, and M. F. Churbanov, Opt. Mater. Express **5**, 1722 (2015).
18. M. Shen, D. Furniss, M. Farries, D. Jayasuriya, Z. Tang, L. Sojka, S. Sujecki, T. M. Benson, and A. B. Seddon, Sci. Rep. **9**, 11426 (2019).
19. M. F. Churbanov, B. I. Denker, B. I. Galagan, V. V. Koltashev, V. G. Plotnichenko, M. V. Sukhanov, S. E. Sverchkov, and A. P. Velmuzhov, Appl. Phys. B **126**, 117 (2020).
20. M. F. Churbanov, B. I. Denker, B. I. Galagan, V. V. Koltashev, V. G. Plotnichenko, G. E. Snopatin, M. V. Sukhanov, S. E. Sverchkov, and A. P. Velmuzhov, J. Non-Cryst. Solids **559**, 120592 (2021).
21. M. F. Churbanov, B. I. Denker, B. I. Galagan, V. V. Koltashev, V. G. Plotnichenko, M. V. Sukhanov, S. E. Sverchkov, and A. P. Velmuzhov, J. Lumin. **231**, 117809 (2021).
22. G. H. Dieke and H. M. Crosswhite, Appl. Opt. **2**, 675 (1963).
23. A. B. Seddon, D. Furniss, Z. Q. Tang, Ł. Sojka, T. M. Benson, R. Caspary, and S. Sujecki, in *18th Int. Conf. on Transparent Opt. Networks (ICTON)* (2016).
24. H. Przybylińska, C.-G. Ma, M. G. Brik, A. Kamińska, P. Sybilski, A. Wittlin, M. Berkowski, Y. Zorenko, V. Gorbenko, H. Wrzesinski, and A. Suchocki, Appl. Phys. Lett. **102**, 241112 (2013).
25. H. Przybylińska, C.-G. Ma, M. G. Brik, A. Kamińska, J. Szczepkowski, P. Sybilski, A. Wittlin, M. Berkowski, W. Jastrzębski, and A. Suchocki, Phys. Rev. B **87**, 045114 (2013).
26. D. W. Coutts and A. S. McGonigle, IEEE J. Quantum Electron. **40**, 1430 (2004).
27. M. Gorjan, M. Marinček, and M. Čopič, IEEE J. Quantum Electron. **47**, 262 (2011).